Brazilian Journal
of Chemical
Engineering

ISSN 0104-6632
Printed in Brazil
www.abeq.org.br/bjche

Vol. 30, No. 01, pp. 187 - 195, January - March, 2013

EFFECTS OF MASS TRANSFER ON MHD FLOW OF CASSON FLUID WITH CHEMICAL REACTION AND SUCTION

S. A. Shehzad[1*], T. Hayat[1], M. Qasim[2] and S. Asghar[2]

[1]Department of Mathematics, Quaid-i-Azam University 45320, Islamabad 44000, Pakistan.
E-mail: ali_qau70@yahoo.com
[2]Department of Mathematics, COMSATS Institute of Information Technology,
Park Road, Chak Shahzad, Islamabad 44000, Pakistan.

(Submitted: January 25, 2012 ; Revised: May 9, 2012 ; Accepted: May 14, 2012)

Abstract - Effect of mass transfer in the magnetohydrodynamic flow of a Casson fluid over a porous stretching sheet is addressed in the presence of a chemical reaction. A series solution for the resulting nonlinear flow is computed. The skin friction coefficient and local Sherwood number are analyzed through numerical values for various parameters of interest. The velocity and concentration fields are illustrated for several pertinent flow parameters. We observed that the Casson parameter and Hartman number have similar effects on the velocity in a qualitative sense. We further analyzed that the concentration profile decreases rapidly in comparison to the fluid velocity when we increased the values of the suction parameter.
Keywords: Casson fluid; Mass transfer; Chemical reaction.

INTRODUCTION

The analysis of boundary layer flow of viscous and non-Newtonian fluids has been the focus of extensive research by various scientists due to its importance in continuous casting, glass blowing, paper production, polymer extrusion, aerodynamic extrusion of plastic sheet and several others. Numerous studies have been presented on various aspects of stretching flows since the seminal work by Crane (1970). One may refer to recent investigations by Hayat and Qasim (2010), Fang *et al*. (2010), Khan and Pop (2010), Ahmad and Asghar (2011), Kandasamy *et al*. (2011), Rashidi *et al*. (2011), Hayat *et al*. (2011), Yao *et al*. (2011) and Makinde and Aziz (2011) in this direction. On the other hand, mass transfer is important due to its appearance in many scientific disciplines that involve convective transfer of atoms and molecules. Examples of this phenomenon are evaporation of water, separation of chemicals in distillation processes, natural or artificial sources etc. In addition, mass transfer with chemical reaction has special significance in chemical and hydrometallurgical industries. The formation of smog represents a first order homogeneous chemical reaction. For instance, one can take into account the emission of NO_2 from automobiles and other smoke-stacks. Thus, NO_2 reacts chemically in the atmosphere with unburned hydrocarbons (aided by sunlight) and produces peroxyacetylnitrate, which forms a layer of photo-chemical smog. Chemical reactions can be treated as either homogeneous or heterogeneous processes. It depends on whether they occur at an interface or as a single-phase volume reaction (Kandasamy *et al*., 2008). A few representative studies dealing with mass transfer in the presence of chemical reaction may be mentioned (Kandasamy *et al*., 2005; Hayat *et al*., 2010; Ziabaksh *et al*., 2010; Makinde, 2010; Ibrahim and Makinde, 2010; Bhattacharyya and Layek, 2011; Hayat *et al*., 2011; Makinde, 2011).

Previous studies on the topic show that little work

*To whom correspondence should be addressed

is presented regarding the effect of mass transfer on the MHD flows of non-Newtonian fluids in the presence of chemical reaction. Constitutive equations of the Casson fluid model (Nakamura and Sawada, 1988; Eldabe and Silwa, 1995; Dash *et al*., 1996; Boyd *et al*., 2007) are employed in the mathematical modeling. The rest of the paper is organized as follows. The next section completes the problem formulation. Then, the next section develops the homotopic solutions. Convergence of the derived series solutions and the discussion of velocity and concentration fields are presented in the sequence. The last section summarizes main points.

GOVERNING PROBLEMS

Consider a magnetohydrodynamic (MHD) and incompressible flow of a Casson fluid over a porous stretching surface at $y = 0$, as shown in Figure 1. We select the Cartesian coordinate system such that the $x-$ axis be taken parallel to the surface and y is perpendicular to the surface. The fluid occupies a half space $y > 0$. The mass transfer phenomenon with chemical reaction is also retained. The flow is subjected to a constant applied magnetic field B_0 in the y direction. The flow is taken to be steady and the magnetic Reynolds number is considered to be very small so that the induced magnetic field is negligible in comparison to the applied magnetic field. The fluid properties are constant.

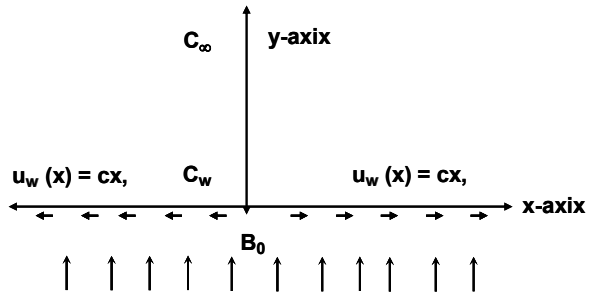

Figure 1: Physical sketch of the problem

The rheological equation of state for an isotropic flow of a Casson fluid can be expressed as (Eldabe and Silwa, 1995):

$$\tau_{ij} = \begin{cases} 2(\mu_B + \frac{p_y}{\sqrt{2\pi}})e_{ij}, \pi > \pi_c, \\ 2(\mu_B + \frac{p_y}{\sqrt{2\pi}})e_{ij}, \pi < \pi_c \end{cases} \quad (1)$$

In the above equation $\pi = e_{ij}e_{ij}$ and e_{ij} denotes the $(i, j)^{th}$ component of the deformation rate, π the product of the component of deformation rate with itself, π_c a critical value of this product based on the non-Newtonian model, μ_B the plastic dynamic viscosity of the non-Newtonian fluid and p_y the yield stress of the fluid. The equations governing the steady boundary layer flow of the Casson fluid are (Mustafa *et al*., 2012)

$$\frac{\partial u}{\partial x} + \frac{\partial v}{\partial y} = 0, \quad (2)$$

$$u\frac{\partial u}{\partial x} + v\frac{\partial u}{\partial y} = \nu(1+1/\beta)\frac{\partial^2 u}{\partial y^2} - \frac{\sigma B_0^2}{\rho}u, \quad (3)$$

$$u\frac{\partial C}{\partial x} + v\frac{\partial C}{\partial y} = D\frac{\partial^2 C}{\partial y^2} - k_1 C \quad (4)$$

along with the following boundary conditions:

$$u = u_w(x) = cx, \ v = -v_0, \ C = C_w \ \text{at} \ y = 0, \quad (5)$$

$$u \to 0, \ C \to C_\infty \ \text{as} \ y \to \infty \quad (6)$$

in which u and v represent the velocity components in the $x-$ and $y-$directions, $\beta = \mu_B\sqrt{2\pi_c}/p_y$ the non-Newtonian Casson parameter, $\nu = (\mu_B/\rho)$ the kinematic viscosity, D the mass diffusion, C the concentration field and k_1 the reaction rate.

Equations (2)-(6) can be made dimensionless by introducing the following change of variables

$$u = cxf'(\eta), \ v = -\sqrt{c\nu}f(\eta), \quad \eta = y\sqrt{\frac{c}{\nu}}, \ \phi = \frac{C - C_\infty}{C_w - C_\infty}. \quad (7)$$

The dimensionless problem satisfies:

$$(1+1/\beta)f''' + ff'' - f'^2 - Mf' = 0, \quad (8)$$

$$\phi'' + Scf\phi' - Sc\gamma\phi = 0, \quad (9)$$

$$f = S, \ f' = 1, \ \phi = 1 \ \text{at} \ \eta = 0, \quad (10)$$

$$f' = 0, \ \phi = 0 \ \text{as} \ \eta \to \infty, \quad (11)$$

where Eq. (2) is satisfied identically, $M = \sigma B_0^2 / \rho c$ the Hartman number, $Sc = \nu / D$ the Schmidt number, $\gamma = k_1 / c$ the chemical reaction parameter and $S = v_0 / \sqrt{\nu c}$ the suction parameter.

The skin friction coefficient and the local Sherwood number can be written as:

$$C_f = \frac{\tau_w}{\rho u_w^2(x)}, \; Sh = \frac{x j_w}{D(C_w - C_\infty)}, \tag{12}$$

in which τ_w is the skin friction (or shear stress along the stretching surface) and j_w the mass flux from the surface, defined by the following relations:

$$\tau_w = \left(\mu_B + \frac{p_y}{\sqrt{2\pi_c}}\right)\left(\frac{\partial u}{\partial y}\right)_{y=0}, \; j_w = -D\left(\frac{\partial C}{\partial y}\right)_{y=0}. \tag{13}$$

Now Eqs. (12) and (13) give:

$$\begin{aligned} &Re_x^{1/2} C_f = (1+1/\beta) f''(0), \\ &Sh / Re_x^{1/2} = -\phi'(0). \end{aligned} \tag{14}$$

HOMOTOPY ANALYSIS SOLUTIONS

The initial guesses and auxiliary linear operators for this problem are selected as follows:

$$f_0(\eta) = S + 1 - \exp(-\eta), \;\; \phi_0(\eta) = \exp(-\eta), \tag{15}$$

$$\mathbf{L}_f = f''' - f', \;\; \mathbf{L}_\phi = f'' - f, \tag{16}$$

such that:

$$\begin{aligned} &\mathbf{L}_f(C_1 + C_2 e^{\eta} + C_3 e^{-\eta}) = 0, \\ &\mathbf{L}_\phi(C_4 e^{\eta} + C_5 e^{-\eta}) = 0, \end{aligned} \tag{17}$$

where C_i $(i = 1-5)$ represent the arbitrary constants. Denoting the nonzero auxiliary parameters $\hbar_f$ and $\hbar_\phi$, the resulting zeroth order problems are developed as follows:

$$\begin{aligned} &(1-p)\mathbf{L}_f\left[\hat{f}(\eta;p) - f_0(\eta)\right] = \\ &p\hbar_f \mathbf{N}_f\left[\hat{f}(\eta;p)\right], \end{aligned} \tag{18}$$

$$\begin{aligned} &(1-p)\mathbf{L}_\phi\left[\hat{\phi}(\eta;p) - \theta_0(\eta)\right] = \\ &p\hbar_\phi \mathbf{N}_\phi\left[\hat{f}(\eta;p), \hat{\phi}(\eta,p)\right], \end{aligned} \tag{19}$$

$$\begin{aligned} &\hat{f}(0;p) = S, \; \hat{f}'(0;p) = 1, \; \hat{f}'(\infty;p) = 0, \\ &\hat{\phi}(0,p) = 1, \; \hat{\phi}(\infty,p) = 0, \end{aligned} \tag{20}$$

where p is an embedding parameter; $\mathbf{N}_f$ and $\mathbf{N}_\phi$ are nonlinear operators which can be defined as:

$$\begin{aligned} \mathbf{N}_f[\hat{f}(\eta,p)] = (1+1/\beta)\frac{\partial^3 \hat{f}(\eta,p)}{\partial \eta^3} + \hat{f}(\eta,p)\frac{\partial^2 \hat{f}(\eta,p)}{\partial \eta^2} \\ - \left(\frac{\partial \hat{f}(\eta,p)}{\partial \eta}\right)^2 - M\,\frac{\partial f(\eta,p)}{\partial \eta}, \end{aligned} \tag{21}$$

$$\begin{aligned} &\mathbf{N}_\phi[\hat{\phi}(\eta,p), \hat{f}(\eta,p)] = \\ &\frac{\partial^2 \hat{\phi}(\eta,p)}{\partial \eta^2} + Sc\hat{f}(\eta,p)\frac{\partial \hat{\phi}(\eta,p)}{\partial \eta} - Sc\gamma\hat{\phi}(\eta,p). \end{aligned} \tag{22}$$

By setting $p = 0$ and $p = 1$ we have:

$$\begin{aligned} &\hat{f}(\eta;0) = f_0(\eta), \; \hat{\phi}(\eta,0) = \phi_0(\eta) \\ &\text{and} \\ &\hat{f}(\eta;1) = f(\eta), \; \hat{\phi}(\eta,1) = \phi(\eta). \end{aligned} \tag{23}$$

We observed that, when p changes from 0 to 1, then $f(\eta,p)$ and $\phi(\eta,p)$ vary from $f_0(\eta), \phi_0(\eta)$ to $f(\eta)$ and $\phi(\eta)$. In view of the Taylor series we can write:

$$f(\eta,p) = f_0(\eta) + \sum_{m=1}^{\infty} f_m(\eta) p^m, \tag{24}$$

$$\phi(\eta,p) = \phi_0(\eta) + \sum_{m=1}^{\infty} \phi_m(\eta) p^m, \tag{25}$$

$$f_m(\eta) = \frac{1}{m!}\frac{\partial^m f(\eta;p)}{\partial \eta^m}\bigg|_{p=0}, \tag{26a}$$

$$\phi_m(\eta) = \frac{1}{m!}\frac{\partial^m \phi(\eta;p)}{\partial \eta^m}\bigg|_{p=0}. \tag{26b}$$

The convergence of the series is strongly dependent upon $\hbar_f$ and $\hbar_\phi$. We select $\hbar_f$ and $\hbar_\phi$ in such a way that the series converge at $p = 1$ and hence:

$$f(\eta) = f_0(\eta) + \sum_{m=1}^{\infty} f_m(\eta), \tag{27}$$

$$\phi(\eta) = \phi_0(\eta) + \sum_{m=1}^{\infty} \phi_m(\eta). \tag{28}$$

The m^{th}-order deformation equations are obtained by differentiating the Equations (18)-(20) m times with respect to p and then putting $p = 0$ to obtain:

$$\mathbf{L}_f[f_m(\eta) - \chi_m f_{m-1}(\eta)] = \hbar_f \mathbf{R}_f^m(\eta), \tag{29}$$

$$\mathbf{L}_\phi[\phi_m(\eta) - \chi_m \phi_{m-1}(\eta)] = \hbar_\phi \mathbf{R}_\phi^m(\eta), \tag{30}$$

$$f_m(0) = f_m'(0) = f_m'(\infty) = 0, \quad \phi_m(0) = \phi_m(\infty) = 0, \tag{31}$$

$$\mathbf{R}_f^m(\eta) = (1 + 1/\beta) f_{m-1}'''(\eta) + \sum_{k=0}^{m-1} \left[f_{m-1-k} f_k'' - f_{m-1-k}' f_k' \right] - M f_{m-1}'(\eta), \tag{32}$$

$$\mathbf{R}_\phi^m(\eta) = \phi_{m-1}'' + Sc \sum_{k=0}^{m-1} f_{m-1-k}' \phi_k' - Sc\gamma \phi_{m-1}, \tag{33}$$

$$\chi_m = \begin{cases} 0, & m \le 1, \\ 1, & m > 1. \end{cases} \tag{34}$$

Our general solutions can be expressed in the form:

$$f_m(\eta) = f_m^*(\eta) + C_1 + C_2 e^{\eta} + C_3 e^{-\eta}, \tag{35}$$

$$\phi_m(\eta) = \phi_m^*(\eta) + C_4 e^{\eta} + C_5 e^{-\eta}, \tag{36}$$

in which f_m^* and ϕ_m^* represent the special solutions.

CONVERGENCE ANALYSIS

The developed series solutions Eqs. (24) and (25) contain $\hbar_f$ and $\hbar_\phi$. The convergence and rate of approximation for the constructed series solutions depend upon these auxiliary parameters. Therefore the $\hbar-$ curves have been plotted for the 20^{th}-order of approximation in order to find the range of admissible values of $\hbar_f$ and $\hbar_\phi$. Fig. 2 shows that the range of admissible values of $\hbar_f$ and $\hbar_\phi$ are $-0.7 \le \hbar_f \le -0.1$ and $-0.8 \le \hbar_\phi \le -0.3$. The series solutions converge in the whole region of η when $\hbar_f = \hbar_\phi = -0.5$. Table 1 shows the convergence of our series solutions for different orders of approximation. It is very clear from this table that 10^{th} order deformations are enough for the velocity whereas 15^{th} order deformations are required for the concentration.

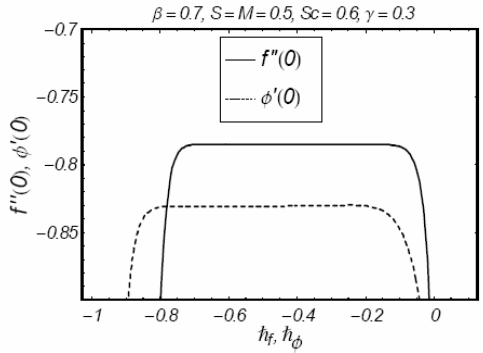

Figure 2: $\hbar-$ curves for the functions β and θ

Table 1: Convergence of the homotopy solution for different orders of approximation when $\beta = 0.6$, $M = 0.5$, $S = 0.5$, $Sc = 0.6$, $\gamma = 0.3$, and $\hbar_f = \hbar_\theta = -0.5$.

Order of approximation	$-f''(0)$	$-\phi'(0)$
1	0.77083	0.92000
10	0.78479	0.82953
15	0.78479	0.83043
20	0.78479	0.83063
35	0.78479	0.83063
40	0.78479	0.83063
45	0.78479	0.83063
50	0.78479	0.83063

RESULTS AND DISCUSSION

The velocity (f') and concentration (ϕ) fields are shown graphically in Figs. 3-10. Figs. 3-5 show the effects of the Casson parameter β, Hartman number M and the suction parameter S, respectively, on the velocity profile $f'(\eta)$. From Fig. 3, we observed that the velocity field decreases when β increases. An increase in β leads to an increase in plastic dynamic viscosity that creates resistance in the flow of fluid and a decrease in fluid velocity is observed. The

effects of Hartman number M and the suction parameter S on $f'(\eta)$ are seen in Figs. 4 and 5. These figs. show that both M and S decrease the velocity $f'(\eta)$. This is due to the fact that the applied magnetic field normal to the flow direction induces the drag in terms of a Lorentz force which provides resistance to flow; suction is an agent which causes resistance to the fluid flow and the fluid velocity also decreased. Figs. 6-10 show the plots of the effects of the Casson parameter β, Hartman number M, suction parameter S, Schmidt number Sc and chemical reaction parameter γ on the concentration field $\phi(\eta)$. The concentration field and associated boundary layer thickness increase when β increases (Fig. 6). It is also noticed from Figs. 3 and 6 that the Casson parameter β has quite opposite effects on the velocity and concentration profiles. Fig. 7 depicts that, by increasing the Hartman number, both the concentration profiles and boundary layer thickness increase. Thus, Hartman number here decreases the resistive force when M increases. The influence of the suction parameter on the concentration profile is seen in Fig. 8. The concentration profile is a decreasing function of S.This is in accordance with the fact that the fluid experiences a resistance upon increasing the friction between its layers. As a consequence, there is a decrease in concentration. Effects of the Schmidt number on $\phi(\eta)$ are displayed in Fig. 9. Here both the concentration profile and the boundary layer thickness decrease when the Schmidt number Sc increases. From a physical point of view, the Schmidt number is dependent on mass diffusion D and an increase in Schmidt number corresponds to a decrease in mass diffusion and the concentration profile reduced. When $\gamma = 0$, there is no chemical reaction. An increase in the chemical reaction parameter corresponds to an increase in the reaction rate parameter and an increase in the reaction rate parameter caused a reduction in concentrarion. From Fig. 10, one can see that an increase in the value of the chemical reaction parameter γ decreased the concentration field $\phi(\eta)$. Figs. 11 and 12 are sketched to visualise the influence of key parameters that are used in the present problems for $Re_x^{1/2} C_f$. The influence of M against β is described in Fig. 11. It is obvious that $Re_x^{1/2} C_f$ is an increasing function of M. Similar effects can be seen in Fig. 12, which shows the influence of β against M. Figs. 13 and 14 are shown to present the influence of sundry parameters on $Sh / Re_x^{1/2}$. Fig. 13 describes the influence of β vs γ on $Sh / Re_x^{1/2}$. This figure confirms that the Sherwood number is a decreasing function of β and the effects on the Sherwood number of γ are the opposite (see Fig. 14). Table 2 shows the skin friction coefficient for the different values of β, M, and S. By increasing the values of β, the value of the skin friction coefficient decreases, but it increases upon increasing M and S Table 3 shows the numerical values of the local Sherwood numbers for the parameters β, M, S, Sc, and γ. This table concludes that the values of the local Nusselt number decrease upon increasing β and M, but increase upon increasing S, Sc and γ. Table 4 shows the comparison with the previous limited studies in the literature. From this table one can see that our series solutions are in excellent agreement with the previous studies, validating the present series solutions.

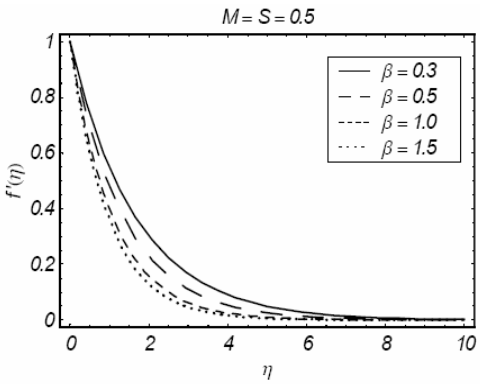

Figure 3: Influence of β on $f'(\eta)$

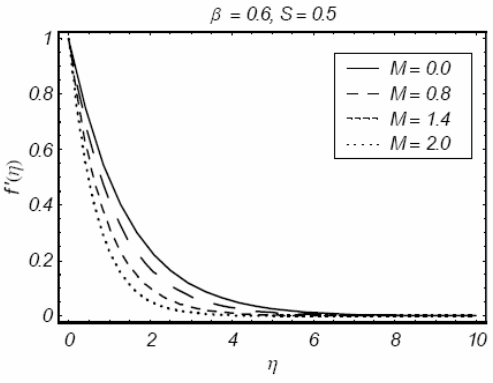

Figure 4: Influence of M on $f'(\eta)$

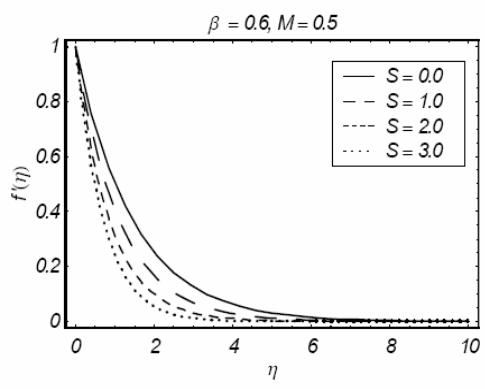

Figure 5: Influence of S on $f'(\eta)$

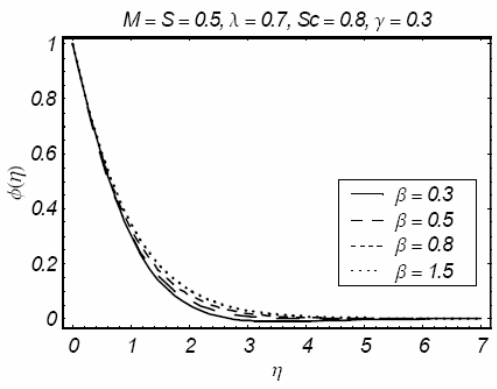

Figure 6: Influence of β on $\phi(\eta)$

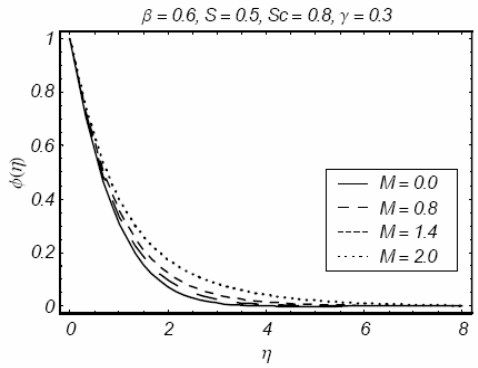

Figure 7: Influence of M on $\phi(\eta)$

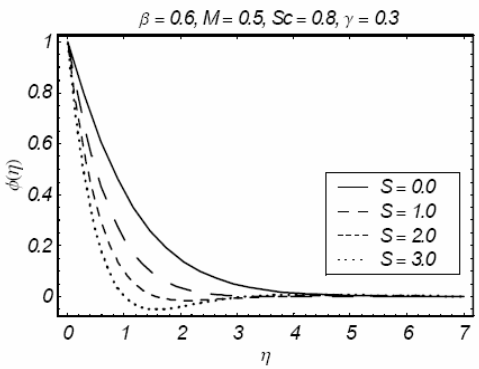

Figure 8: Influence of S on $\phi(\eta)$

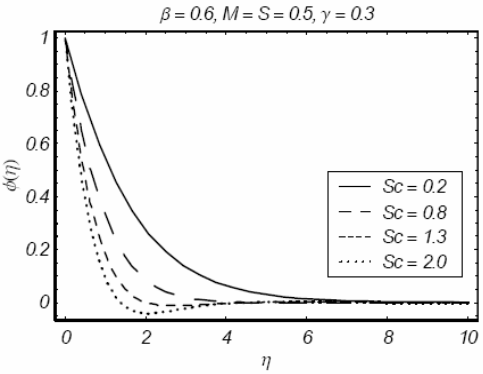

Figure 9: Influence of Sc on $\phi(\eta)$

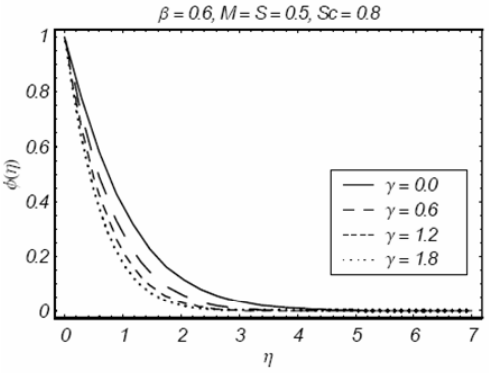

Figure 10: Influence of γ on $\phi(\eta)$

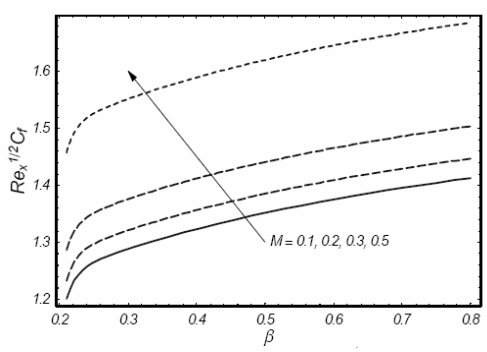

Figure 11: Influence of M on $Re_x^{1/2} C_f$ vs β

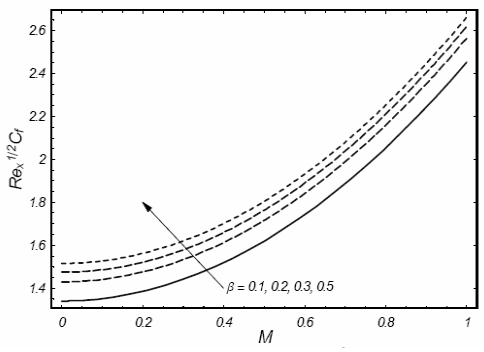

Figure 12: Influence of β on $Re_x^{1/2} C_f$ vs M.

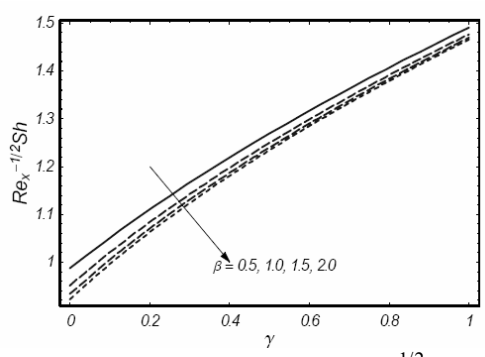

Figure 13: Influence of β on $Sh / Re_x^{1/2}$ vs γ.

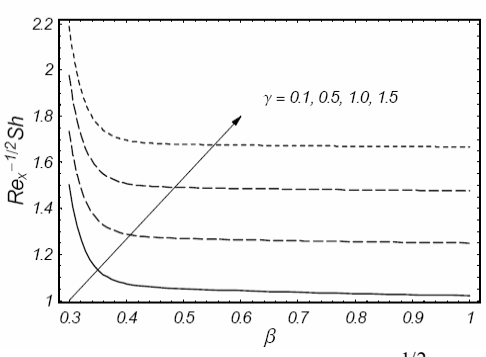

Figure 14: Influence of γ on $Sh / Re_x^{1/2}$ vs β

Table 2: **Numerical values of the skin-friction coefficient $(1+1/\beta)f''(0)$ for different values of β, M and S.**

β	M	S	$-(1+1/\beta)f''(0)$
0.5	0.5	0.5	2.20256
0.8			1.94558
1.3			1.75799
2.0			1.64195
0.8	0.0		1.77069
	0.6		2.01706
	1.2		2.60638
	1.5		2.96570
		0.0	1.67705
		0.7	2.06318
		1.4	2.51728
		2.0	2.95256

Table 3: Numerical values of the local Sherwood number $-\phi'(0)$ for different values of β, M, S, Sc and γ.

β	M	S	Sc	γ	$-\phi'(0)$
0.5	0.5	0.5	0.6	0.3	0.836083
0.9					0.819149
1.4					0.808194
2.0					0.800845
0.7	0.0				0.834056
	0.7				0.819545
	1.2				0.799472
	1.6				0.782899
		0.0			0.635925
		0.4			0.785992
		1.0			1.04054
		2.0			1.52177
			0.4		0.627639
			0.8		1.00620
			1.3		1.41079
			2.0		1.91726
				0.0	0.672845
				0.4	0.869844
				0.7	0.987078
				1.0	1.08953

Table 4: Comparison of values of $-\phi'(0)$ for different values of γ when $\beta \to \infty$ and M = S = 0.0.

γ	Sc	Saleem ans El – Aziz (2008)	Andersson *et al.* (1994)	Present results
0.01	1.0	-0.592	-0.59157	0.59136
0.1	1.0	-0.669	-0.66902	0.66898
1.0	1.0	-1.177	-1.17649	1.17650
10	1.0	-3.232	-3.23122	-3.23175

CONCLUSIONS

Effects of mass transfer on the MHD boundary layer flow of a Casson fluid model with chemical reaction are addressed. The present analysis leads to the following observations.

- The Casson parameter β and Hartman number M have similar effects on the velocity profile $f'(\eta)$.
- β has opposite effects on the velocity and concentration profiles.
- The concentration field $\phi(\eta)$ as well as the boundary layer thickness increase upon increasing the Hartman number M.
- An increase in the Schmidt number Sc causes a decrease in the concentration profile and the boundary layer thickness.
- When $\gamma = 0$, there is no chemical reaction. An increase in γ decreases $\phi(\eta)$.

REFERENCES

Ahmad, A. and Asghar, S., Flow of a second grade fluid over a sheet stretching with arbitrary velocities subject to a transverse magnetic field. Applied Math. Letters 24, p. 1905 (2011).

Andersson, H. I., Hansen, O. R. and Holmedal, B., Diffusion of a chemically reactive species from a stretching sheet. Int. J. Heat Mass Transfer, 37, p. 659 (1994).

Bhattacharyya, K. and Layek, G. C., Slip effect on diffusion of chemically reactive species in boundary layer flow over a vertical stretching sheet with suction or blowing. Chemical Eng. Commun., 198, p. 1354 (2011).

Boyd, J., Buick, J. M. and Green, S., Analysis of the Casson and Carreau-Yasuda non-Newtonian blood models in steady and oscillatory flow using the lattice Boltzmann method. Phys. Fluids, 19, p. 93 (2007).

Crane, L. J., Flow past a stretching plate. Z. Angew. Math. Mech., 21, p. 645 (1970).

Dash, R. K., Mehta, R. K. and Jayarama, G., Casson fluid flow in a pipe filled with a homogenous porous medium. Int. J. Eng. Sci., 34, p. 1145 (1996).

Eldabe, N. T. M. and Salwa, M. G. E., Heat transfer of MHD non-Newtonian Casson fluid flow between two rotating cylinders. J. Phys. Soc. Japan, 64, p. 41 (1995).

Fang, T., Zhang, J. and Yao, S., A new family of unsteady boundary layers over a stretching surface. Appl. Math. Comput., 217, p. 3747 (2010).

Hayat, T. and Qasim, M., Influence of thermal radiation and Joule heating on MHD flow of a Maxwell fluid in the presence of thermophoresis. Int. J. Heat Mass Transfer, 53, p. 4780 (2010).

Hayat, T., Qasim, M., Abbas, Z. and Hendi, A. A., Magnetohydrodynamic flow and mass transfer of a Jeffery fluid over a nonlinear stretching surface. Z. Naturforsch A, 64a, p. 1111 (2010).

Hayat, T., Shehzad, S. A. and Qasim, M., Mixed convection flow of a micropolar fluid with radiation and chemical reaction. Int. J. Num. Methods Fluids, 67, p. 1418 (2011).

Hayat, T., Shehzad, S. A., Qasim, M. and Obaidat, S., Steady flow of Maxwell fluid with convective boundary conditions. Z. Naturforsch., 66a, p. 417 (2011).

Ibrahim, S. Y. and Makinde, O. D., Chemically reacting MHD boundary layer flow of heat and mass transfer past a moving vertical plate with suction. Scientific Research Essays, 5, p. 2875 (2010).

Kandasamy, R., Loganathan, P. and Arasu, P. V., Scaling group transformation for MHD boundary-layer flow of a nanofluid past a vertical stretching surface in the presence of suction/injection. Nuclear Engineering and Design, 241, p. 2053 (2011).

Muhaimin, I., Kandasamy, R., Hashim, I., Thermophoresis and chemical reaction effects on non-Darcy MHD mixed convective heat and mass transfer past a porous wedge in the presence of variable stream condition. Chem. Eng. Research Design, 87, p. 1527 (2009).

Kandasamy, R., Periasamy, K. and Prabhu, K. K. S., Chemical reaction, heat and mass transfer on MHD flow over a vertical stretching surface with heat source and thermal stratification effects. Int. J. Heat Mass Transfer, 48, p. 4751 (2005).

Khan, W. A. and Pop, I., Boundary flow of a nano-fluid past a stretching sheet. Int. J. Heat Mass Transfer, 53, p. 2477 (2010).

Makinde, O. D. and Aziz, A., Boundary layer flow of a nano fluid past a stretching sheet with convective boundary conditions. Int. J. Thermal. Sci., 50, p. 1326 (2011).

Makinde, O. D., MHD mixed-convection interaction with thermal radiation and nth order chemical reaction past a vertical porous plate embedded in a porous medium. Chem. Eng. Commun., 198, p. 590 (2011).

Makinde, O. D., Similarity solution of hydromagnetic heat and mass transfer over a vertical plate with a convective surface boundary condition. Int. J. Physical Sci., 5, p. 700 (2010).

Mustafa, M., Hayat, T., Pop, I. and Hendi, A. A., Stagnation-point flow and heat transfer of a Casson fluid towards a stretching sheet. Z. Naturforsch., 67a, p.70 (2012).

Nakamura, M. and Sawada, T., Numerical study on the flow of a non-Newtonian fluid through an axisymmetric stenosis. ASME J. Biomech. Eng., 110, p.137 (1988).

Rashidi, M. M., Mohimanian pour, S. A. and Abbasbandy, S., Analytic approximate solutions for heat transfer of a micropolar fluid through a porous medium with radiation. Commun. Nonlinear Sci. Numer. Simulat., 16, p. 1874 (2011).

Salem, A. M. and El-Aziz, M. A., Effect of Hall currents and chemical reaction on hydromagnetic flow of a stretching vertical surface with internal heat generation/absorption. Appl. Mathematical Modelling, 32, p. 1236 (2008).

Yao, S., Fang, T. and Zhong, Y., Heat transfer of a generalized stretching/shrinking wall problem with convective boundary conditions. Commun. Nonlinear Sci. Numer. Simulat., 16, p. 752 (2011).

Ziabakhsh, Z., Domairry, G., Bararnia, H. and Babazadeh, H., Analytical solution of flow and diffusion of chemically reactive species over a nonlinearly stretching sheet immersed in a porous medium. J. Taiwan Institute Chemical Eng., 41, p. 22 (2010).